



Nonclassical Monocytes Are Prone to Migrate Into Tumor in Diffuse Large B-Cell Lymphoma

Simon Le Gallou, Faustine Lhomme, Jonathan M Irish, Anna Mingam, Celine Pangault, Celine Monvoisin, Juliette Ferrant, Imane Azzaoui, Delphine Rossille, Krimo Bouabdallah, et al.

► To cite this version:

Simon Le Gallou, Faustine Lhomme, Jonathan M Irish, Anna Mingam, Celine Pangault, et al.. Non-classical Monocytes Are Prone to Migrate Into Tumor in Diffuse Large B-Cell Lymphoma. *Frontiers in Immunology*, 2021, 12, pp.755623. 10.3389/fimmu.2021.755623 . hal-03531047

HAL Id: hal-03531047

<https://hal.science/hal-03531047>

Submitted on 2 Jun 2022

HAL is a multi-disciplinary open access archive for the deposit and dissemination of scientific research documents, whether they are published or not. The documents may come from teaching and research institutions in France or abroad, or from public or private research centers.

L'archive ouverte pluridisciplinaire **HAL**, est destinée au dépôt et à la diffusion de documents scientifiques de niveau recherche, publiés ou non, émanant des établissements d'enseignement et de recherche français ou étrangers, des laboratoires publics ou privés.



Distributed under a Creative Commons Attribution 4.0 International License



Nonclassical Monocytes Are Prone to Migrate Into Tumor in Diffuse Large B-Cell Lymphoma

Simon Le Gallou^{1,2†}, Faustine Lhomme^{1,3†}, Jonathan M. Irish^{3,4}, Anna Mingam¹, Celine Pangault^{1,2}, Celine Monvoisin², Juliette Ferrant², Imane Azzaoui¹, Delphine Rossille^{1,2}, Krime Bouabdallah⁵, Gandhi Damaj⁶, Guillaume Cartron⁷, Pascal Godmer⁸, Steven Le Gouill⁹, René-Olivier Casasnovas¹⁰, Thierry Jo Molina¹¹, Roch Houot^{2,12}, Thierry Lamy^{2,12}, Karin Tarte^{1,2}, Thierry Fest^{1,2} and Mikael Roussel^{1,2*}

OPEN ACCESS

Edited by:

Sven Brandau,
University of Duisburg-Essen,
Germany

Reviewed by:

Marc Seifert,
Essen University Hospital, Germany
Gero Knittel,
Essen University Hospital, Germany
Loems Ziegler-Heitbrock,
Independent Researcher,
Munich, Germany

*Correspondence:

Mikael Roussel
mikaël.roussel@univ-rennes1.fr

[†]These authors have contributed
equally to this work

Specialty section:

This article was submitted to
Cancer Immunity
and Immunotherapy,
a section of the journal
Frontiers in Immunology

Received: 09 August 2021

Accepted: 24 November 2021

Published: 16 December 2021

Citation:

Le Gallou S, Lhomme F, Irish JM, Mingam A, Pangault C, Monvoisin C, Ferrant J, Azzaoui I, Rossille D, Bouabdallah K, Damaj G, Cartron G, Godmer P, Le Gouill S, Casasnovas R-O, Molina TJ, Houot R, Lamy T, Tarte K, Fest T and Roussel M (2021) Nonclassical Monocytes Are Prone to Migrate Into Tumor in Diffuse Large B-Cell Lymphoma. *Front. Immunol.* 12:755623. doi: 10.3389/fimmu.2021.755623

¹ Centre Hospitalier Universitaire de Rennes, Pôle Biologie, Rennes, France, ² Institut National de la Santé et de la Recherche Médicale, Unité Mixte de Recherche U1236, Université Rennes 1, Etablissement Français du Sang Bretagne, Rennes, France, ³ Department of Cell and Developmental Biology, Vanderbilt University School of Medicine, Nashville, TN, United States, ⁴ Department of Pathology, Microbiology and Immunology, Vanderbilt University School of Medicine, Nashville, TN, United States, ⁵ Centre Hospitalier Universitaire de Bordeaux, Service d'Hématologie Clinique, Bordeaux, France, ⁶ Centre Hospitalier Universitaire de Caen, Service d'Hématologie Clinique, Caen, France, ⁷ Centre Hospitalier Universitaire de Montpellier, Service d'Hématologie Clinique, Montpellier, France, ⁸ Centre Hospitalier de Bretagne Atlantique, Unité d'Hématologie Clinique, Vannes, France, ⁹ Centre Hospitalier Universitaire de Nantes, Service d'Hématologie Clinique, Institut National de la Santé et de la Recherche Médicale, Centre de Recherche en Cancérologie et Immunologie Nantes Angers (INSERM CCRCINA) Nantes-Angers, NeXT Université de Nantes, Nantes, France, ¹⁰ Centre Hospitalier Universitaire de Dijon, Service d'Hématologie Clinique, Dijon, France, ¹¹ Assistance Publique, Hôpitaux de Paris (APHP), Necker, Service d'Anatomopathologie, Sorbonne Université, Paris, France, ¹² Centre Hospitalier Universitaire de Rennes, Service d'Hématologie Clinique, Rennes, France

Absolute count of circulating monocytes has been proposed as an independent prognostic factor in diffuse large B-cell lymphoma (DLBCL). However, monocyte nomenclature includes various subsets with pro-, anti-inflammatory, or suppressive functions, and their clinical relevance in DLBCL has been poorly explored. Herein, we broadly assessed circulating monocyte heterogeneity in 91 DLBCL patients. Classical- (cMO, CD14^{pos} CD16^{neg}) and intermediate- (iMO, CD14^{pos} CD16^{pos}) monocytes accumulated in DLBCL peripheral blood and exhibited an inflammatory phenotype. On the opposite, nonclassical monocytes (ncMOSlan^{pos}, CD14^{low} CD16^{pos} Slan^{neg} and ncMOSlan^{neg}, CD14^{low} CD16^{pos}, Slan^{neg}) were decreased in peripheral blood. Tumor-conditioned monocytes presented similarities with ncMO phenotype from DLBCL and were prone to migrate in response to CCL5 and CXCL12, and presented similarities with DLBCL-infiltrated myeloid cells, as defined by mass cytometry. Finally, we demonstrated the adverse value of an accumulation of nonclassical monocytes in 2 independent cohorts of DLBCL.

Keywords: B cell lymphoma, DLBCL, biomarker, monocyte, immune suppression

INTRODUCTION

Circulating monocytes are classified by their CD14 and CD16 expression as classical- (cMO, CD14^{pos} CD16^{neg}), intermediate- (iMO, CD14^{pos} CD16^{pos}), and nonclassical- monocytes (ncMO, CD14^{low} CD16^{pos}) (1). In addition, Slan expression [6-Sulfo LacNac, which is a carbohydrate modification of P-selectin glycoprotein ligand-1 (PSGL-1)], allows the sub-classification of ncMO Slan^{pos} (CD14^{low}

CD16^{pos} Slan^{pos}) and ncMO Slan^{neg} (CD14^{low} CD16^{pos} Slan^{neg}) (2, 3). Lastly monocytic myeloid derived suppressor cells (M-MDSC, CD14^{pos} HLA-DR^{low}) found in acute or chronic inflammatory context, including cancers, are defined by an impairment of T- and NK- effector functions (4). This nomenclature reflects pro-inflammatory, anti-inflammatory, or suppressive functions described for monocytes (5, 6).

In diffuse large B-cell lymphoma (DLBCL), tumor microenvironment (TME), myeloid cells are supportive of the neoplastic process (7–10). In blood from DLBCL patients, an increase in circulating monocytes is a marker of adverse prognosis (11–15). However, so far monocytes were considered as a whole, and few studies analyzed the monocyte subsets and their clinical relevance even if their intrinsic functions are known to be different. Among monocyte subsets: i) Slan^{pos} monocytes were increased and displayed high rituximab mediated antibody-dependent cellular cytotoxicity (16); ii) an increase in CD16^{pos} or CD11b^{pos}CX3CR1^{pos} monocytes predicted poor progression free- and overall- survival (17, 18); iii) CD14^{pos}CD163^{pos}PD-L1^{pos} monocytes were increased (19); and finally iv) functional M-MDSCs were enriched in peripheral blood and predicted poor event-free survival (20–22). In DLBCL tumor, the myeloid compartment heterogeneity was recently approached by high dimensional analysis revealing distinct macrophage phenotype across lymphoma subtypes (23).

In light with the observation that various monocyte subsets are involved in the biology of DLBCL, we investigated the canonical cMO, iMO, ncMO Slan^{pos}, and ncMO Slan^{neg} subsets in two large cohorts of patients. We quantified these subsets, analyzed their phenotype and functions as well as the clinical relevance of these cells. We found here that in DLBCL, ncMO are prone to migrate into tissues and that their increase in peripheral blood is associated with an adverse prognosis.

METHODS

Samples

A cohort of 91 DLBCL patients at diagnosis from the BMS-LyTRANS clinical trial (ClinicalTrials.gov Identifier: NCT01287923) was used in this study. Clinical characteristics of DLBCL patients enrolled in this training cohort are listed in **Table 1**. Patients with previous corticosteroid treatment were excluded from this study. As controls, age-matched healthy donors (HD, n = 49), follicular lymphomas (n = 9), mantle cell lymphomas (n = 9), chronic lymphocytic leukemias (n = 11), and marginal zone lymphomas (n = 10) were included. Part of these samples (DLBCL and HD) were used in a previous work (22). Prognosis scores were validated in a second cohort of 155 DLBCL patients from the recently published GAINED trial (ClinicalTrials.gov Identifier: NCT01659099) (24). Clinical characteristics of DLBCL patients enrolled in this validation cohort are listed in **Table 1**. The research protocol was conducted under French legal guidelines and fulfilled the requirements of the local institutional ethics committee and biosecurity procedures.

Fluorescent Flow Cytometry Analysis

Blood samples were collected on heparin tubes. Flow cytometry analysis of M-MDSCs, cMO, iMO, and ncMO were performed on whole blood (300 µL/tube) with the antibody panel shown **Table S1** and the gating strategy defined **Figure S1**. Absolute counts were obtained by using Flow-Count beads (Beckman Coulter, Brea, CA). An erythrocytes lysis (Uti-Lyse Dako, Carpinteria, CA) was performed before analysis by flow cytometry (Navios, Beckman Coulter). Analyses were performed using Kaluza software (Beckman Coulter).

In Vitro Culture

OCI-Ly3 and OCI-Ly19 cell lines were cultured in OCI-Ly medium (IMDM supplemented with 10% human AB serum, 1% penicillin-streptomycin (Invitrogen) and 50 µM of β-Mercaptoethanol). For supernatants, OCI-Ly 3 and 19 were seeded at 3 x 10⁶ cells/ml in OCI-Ly medium for 24h (37°C, 5% CO₂). Supernatants were obtained after centrifugation and were frozen at -80°C until migration assay. For control of migration assay, OCI-Ly medium were incubated at (37°C, 5% CO₂) without cells for 24h before centrifugation and freezing.

Monocytes were obtained from PBMCs by elutriation before cryopreservation (plate-forme DTC; CIC Biotherapie, Nantes, France). Monocytes were thawed and resuspended at 4 x 10⁶ cells/mL in RPMI 1640 (Invitrogen, Carlsband, CA, USA) supplemented with 10% FCS and antibiotics (Invitrogen) and then diluted at 2 x 10⁶ cells/mL by adding, as control, the OCI-Ly medium (IMDM supplemented with 10% human AB serum, 1% penicillin-streptomycin and 50 µM of β-Mercaptoethanol, or OCI-Ly3 or OCI-Ly19 supernatant. Two mL of cell suspension were seeded in a 6-well plate during 4 days before mass cytometry analysis or migration assay.

Mass Cytometry Analysis

Cell labeling and mass-cytometry analysis were performed as previously described. (25–27) Briefly, cells were incubated with 25 µM cisplatin (Fluidigm San Francisco, CA, USA). Then, 5 x 10⁶ cells were washed in PBS (HyClone Laboratories, Logan, UT, USA) containing 1% BSA (Thermo Fisher Scientific) and stained in 100 µL PBS and BSA 1%-containing Antibody cocktail. Cells were stained for 30 min at RT with the antibodies (**Table S2**) Cells were washed twice in PBS - BSA 1% before fixation in 1.6% PFA, and permeabilization with methanol (Electron Microscopy Sciences, Hatfield, PA, USA). After incubating overnight at -20°C in MeOH, cells were washed twice with PBS -BSA 1% and stained 20 min with iridium intercalator (Fluidigm, Sunnyvale, CA, US). Finally, cells were washed twice with PBS and twice with diH2O before acquisition a CyTOF 2.0 mass cytometer (Fluidigm). Mass cytometry raw data were deposited in Flow Repository (<http://flowrepository.org/id/FR-FCM-Z4N6>).

Data Processing and Analysis

Data analysis was performed using the workflow previously developed (23). Briefly, after acquisition, intrafile signal drift was normalized and fcs files were obtained using CyTOF

TABLE 1 | Patient's characteristics at baseline.

| | Healthy donors (n = 49) | BMS-LyTRANSTraining cohort (n = 91) | GAINED (24) Validation cohort (n = 155) |
|--|-------------------------|-------------------------------------|---|
| Average age, years (range) | 52.9 (25-66) | 55.7 (18-83) | 44.9 (19-60) |
| Male, n (%) | 30 (61.2%) | 56 (61.5%) | 86 (55.5%) |
| Female, n (%) | 19 (38.8%) | 35 (38.5%) | 69 (44.5%) |
| aalPI, n (%) | | | |
| 0 to 1 | NA | 46 (59%)* | 68 (43.9%) |
| 2 | NA | 28 (35.9%)* | 71 (45.8%) |
| 3 | NA | 4 (5.1%)* | 16 (10.3%) |
| Cell of origin, n (%) | | | |
| GCB (Hans [§] or Nanostring [®]) | NA | 30 (54.5%)*, & | 83 (74.8%)*, & |
| Non-GCB (Hans [§]) or ABC (Nanostring [®]) | NA | 25 (45.5%)*, & | 28 (25.2%)*, & |
| Unclassified [®] | NA | NA | 9 [®] |
| Insufficient material | NA | 36 | 35 |
| Chemotherapy, n | | | |
| Rituximab CHOP | NA | 69 | 37 |
| Rituximab ACVBP | NA | 0 | 39 |
| Obinutuzumab CHOP | NA | 6 | 40 |
| Obinutuzumab ACVBP | NA | 0 | 38 |
| Other treatment | NA | 3 | 0 |
| Unknown or not treated | NA | 13 | 1 |

aalPI, age adjusted International prognostic index; GCB, germinal center B cell; ABC, activated B cell *percentage among cases with known data; [§]defined by Hans algorithm; [®]defined by nanostring analysis. CHOP, cyclophosphamide, doxorubicine, vincristine, and prednisone; ACVBP, doxorubicine, prednisone, cyclophosphamide, vindesine, and bleomycine; NA, not applicable.

software. To diminish batch effects, all files were normalized on EQ Beads (Fluidigm) using the premissa R package (<https://github.com/ParkerICI/premissa>). Raw median intensity values were transformed to a hyperbolic arcsine (arcsinh) and then analysis was performed using Cytobank software (Beckman Coulter, Brea, CA, USA).

Migration Assay

At day 4 of monocyte culture with OCI-Ly3, or OCI-Ly19 supernatant, or control culture medium, cells were collected and washed twice in PBS before starvation during 1 hour (37°C, 5% CO₂) at 10⁶ cells/mL in RPMI 1% HSA. Then, cells were washed once, counted and 100 µL of cells at 10⁶ cells/mL were added to the upper compartment of Transwell chambers with 5 µm pore filters (Corning Incorporated, Kennebunk, ME, USA). The lower chamber contained a chemokine among CCL2 (R&D Systems, 30 ng/ml), CCL3 (R&D Systems, 20 ng/ml), CCL5 (R&D Systems, 30 ng/ml), CCL22 (R&D Systems, 20 ng/ml), CXCL5 (R&D Systems, 20 ng/ml), CXCL12 (R&D Systems, 20 ng/ml), or RPMI 1640 1% HSA as control (corresponding to Basal migration). Cells in the lower chamber were collected after 5h (37°C, 5% CO₂) and the absolute number of viable (DAPI negative) monocytes was quantified by flow cytometry using Precision Count BeadsTM (Biolegend Inc, San Diego, CA, USA). The absolute number of cells (Total Cells) added to the upper compartment at the beginning of migration assay was also determined for each condition (control, OCI-Ly3 and OCI-Ly19) with Precision Count BeadsTM. Percentage of cells that have specifically migrated against a chemokine was calculated as follow: Specific migration = (Lower chamber - Basal migration)/Total cells x 100. The migration represents the variation of this percentage with OCI-Ly supernatants compared to control culture medium (% of specific migration with supernatant – % of specific migration with medium) for each chemokine.

Cell Sorting

cMO (CD19^{neg} CD3^{neg} CD335^{neg} CD45^{pos} CD14^{high} CD16^{neg}), iMO (CD19^{neg} CD3^{neg} CD335^{neg} CD45^{pos} CD14^{high} CD16^{pos}), ncMO Slan^{pos} (CD19^{neg} CD3^{neg} CD335^{neg} CD45^{pos} CD14^{low} CD16^{pos} Slan^{pos}), and ncMO Slan^{neg} (CD19^{neg} CD3^{neg} CD335^{neg} CD45^{pos} CD14^{low} CD16^{pos} Slan^{neg}) were sorted from thawed PBMC of DLBCL patients and HD using an ARIA II (FACSaria, BD Biosciences).

Quantitative Real-Time PCR

Total RNA was extracted using Nucleospin[®] RNA XS kit (Macherey-Nagel, Duren, Germany). cDNA was then generated using Fluidigm Reverse Transcription Master Mix (Fluidigm). The qPCR were performed in triplicate using 96.96 Dynamic ArrayTM IFCs and the BioMarkTM HD System from Fluidigm. For each sample, the mean CT value for the gene of interest was calculated, normalized to the geometric mean value of the 2 housekeeping genes (*CDKN1B* and *ELF1*) (Table S3), and compared to the median value obtained from the reference population (HD cMO or iMO, and DLBCL ncMO) using the 2-ddCT method. Results were expressed as the ratio of sample mean to reference mean for each gene.

Statistical Analysis

Statistical analyses were performed with GraphPad Prism 8.4.3 software (GraphPad Software, San Diego, CA, USA) using Pearson correlation, Wilcoxon, Mann-Whitney, Ordinary one-way ANOVA with Tukey's multiple comparisons test, and Fishers's exact tests as appropriate. Optimal thresholds were defined with the *maxstat* package, log-rank tests were performed with the *survminer* package, cox model for univariate and multivariate analysis were performed with the *survival* package. Analyses were generated with R v4.0.3, using Rstudio v1.3.1093.

Data Sharing Statement

For original data, please contact the corresponding author. Mass cytometry raw data were deposited in Flow Repository (<http://flowrepository.org/id/FR-FCM-Z4N6>). QPCR raw data are included in **Table S4**.

RESULTS

cMO and iMO Are Increased in DLBCL

We have previously shown that M-MDSCs accumulated in DLBCL peripheral blood (22). However, this increase accounts for only a part of the total monocyte accumulation suggesting that additional monocyte subsets are also increased in DLBCL samples (**Figure 1A**). We quantified the absolute count of the 4 circulating monocyte subsets M-MDSC, cMO, iMO, and ncMO. M-MDSC, cMO, and iMO were increased in DLBCL when compared to HDs ($P < .05$, median: 5.75×10^6 cells/L vs 2.8×10^6 cells/L, 348.8×10^6 cells/L vs 274.1×10^6 cells/L, and 34.4×10^6 cells/L vs 26.1×10^6 cells/L; respectively). Conversely, ncMO were significantly decreased in DLBCL when compared to HD

($P < .0001$, median: 17.1×10^6 cells/L vs 36.1×10^6 cells/L; **Figure 1B**). Noteworthy, whereas the increase of cMO and iMO was also found in other B cell lymphomas, this decrease in ncMO was specific of DLBCL (**Figure S2**). Then, we wondered in which monocyte subset M-MDSCs were included. Of note M-MDSC count was correlated with total monocyte ($R = .57$, $P < .0001$), cMO ($R = .61$, $P < .0001$), but was not correlated with iMO and ncMO (**Figure 1C**). No correlation were observed between MO subsets in HD samples (data not shown). Regarding CD14 and CD16 expression, M-MDSCs were essentially aligned with the cMO phenotype and to a lesser extent to iMO (**Figure 1D**). Altogether, these results confirmed that in addition to MDSCs, cMO and iMO were also involved in the monocyte increase observed in DLBCL patients.

DLBCL cMO and iMO Share a Common Inflammatory Phenotype

To further identify the immune properties of monocyte subsets, we sorted cMO and iMO from DLBCL ($n=7$) and HD ($n=4$) samples. Gene expression was assessed by high throughput qPCR on 71 genes involved in myeloid biology (22)

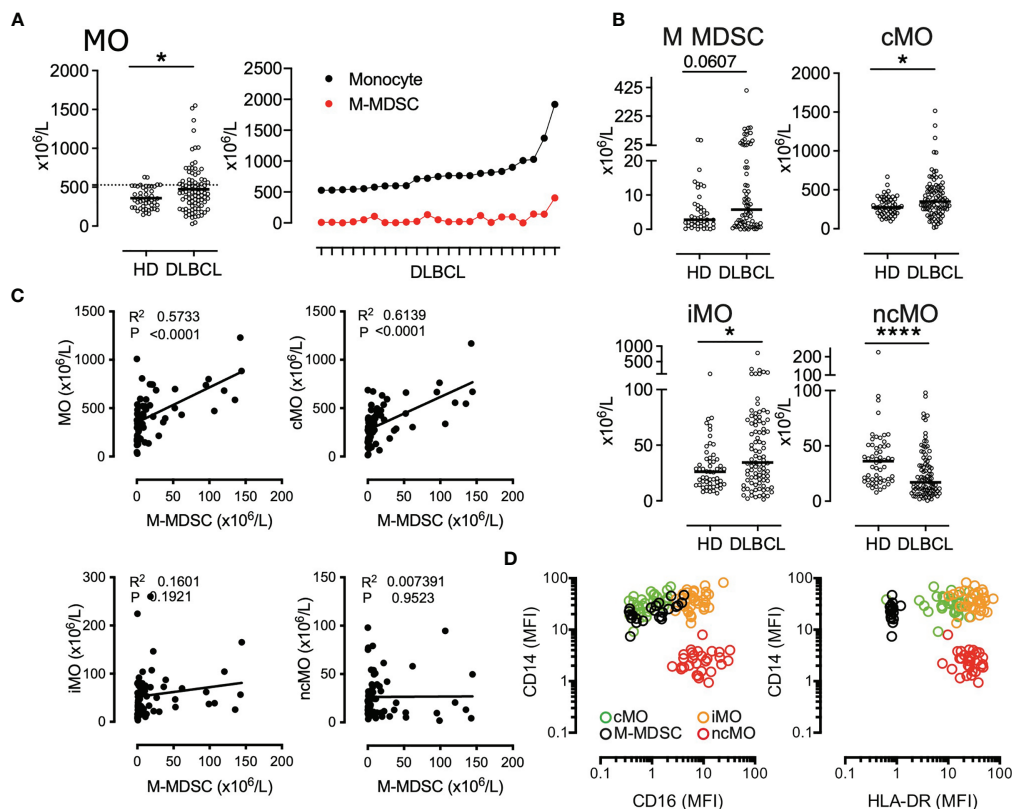


FIGURE 1 | cMO and iMO are increased in peripheral blood from DLBCL. **(A)** Monocyte absolute counts in HD ($n = 49$) and DLBCL ($n = 88$). For the 23 DLBCL samples with monocyte above 528×10^6 monocytes/L (corresponding to the 90th percentile of HD), proportion of M-MDSC within monocyte **(B)** M-MDSC in HD ($n = 43$) and DLBCL ($n = 69$) and monocyte subset counts [classical- (cMO), intermediate- (iMO), and nonclassical- (ncMO)] in peripheral blood from HD ($n = 55$) and DLBCL patients ($n = 91$). **(C)** Pearson correlation between M-MDSC and monocyte (MO), cMO, iMO, and ncMO ($n = 68$). **(D)** Mean fluorescent intensity (MFI) for CD14, CD16, and HLA-DR. Each dot represents a DLBCL sample ($n = 33$) colored by monocyte subset (MDSC, cMO, iMO, and ncMO). Mann-Whitney test were performed. * $P < .05$, **** $P < .0001$.

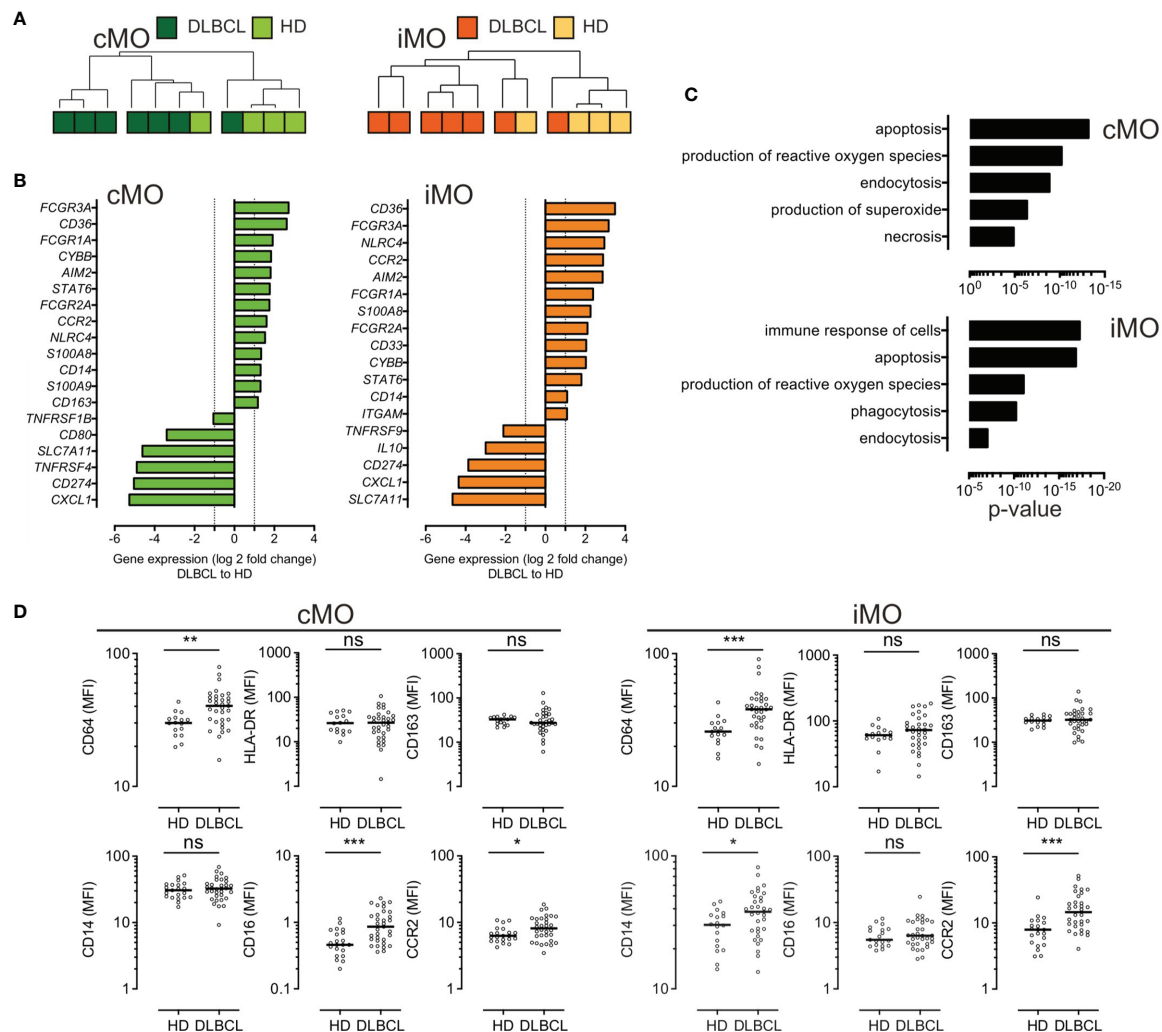


FIGURE 2 | Circulating cMO and iMO share a common inflammatory phenotype, in DLBCL. **(A)** Unsupervised hierarchical clustering of classical- (cMO) and intermediate- (iMO) monocytes, from HD (n = 4) and DLBCL (n = 7) samples. See **Table S3** for a list of genes analyzed on monocyte subsets after cell sorting. Pearson's correlation and complete linkage was employed. **(B)** Transcripts differentially expressed ($P < .05$; $|\log_2FC| > 1$) between DLBCLs and HDs, for cMO and iMO. **(C)** Predicted top 5 biological processes increased for cMO and iMO from DLBCL (Ingenuity Pathway Analysis, z-score > 2.5 , ranked by p-value). **(D)** Mean fluorescence (MFI) for CD64, HLA-DR, CD163, CD14, CD16, and CCR2 for HD (n = 16) and DLBCL (n = 33) samples. Mann-Whitney test were performed. * $P < .05$, ** $P < .01$, *** $P < .001$, ns, non-significant.

(**Tables S3, S4**, and **Figure S3**). Of note, 6 cMO and 5 iMO out of 7 DLBCL were clustered (**Figure 2A** and **Figure S3**). DLBCL cMO and DLBCL iMO were significantly enriched for inflammatory genes (*FCGR3A*, *CD36*, *FCGR1A*, *CYBB*, *AIM2*, *STAT6*, *FCGR2A*, *CCR2*, *NLRC4*, *S100A8*, and *CD14* genes), when compared to the corresponding subsets in HDs ($P < .05$, $|\log_2FC| > 1$) (**Figure 2B**). In addition, *S100A9* and *CD163* were also increased in DLBCL cMO, whereas *CD33* and *ITGAM* were enriched only in DLBCL iMO. For both subsets, *SLC7A11*, *CD274*, and *CXCL1* were expressed at lower levels in DLBCLs (**Figure 2B**). Biological processes enriched in DLBCL cMO and iMO included apoptosis, production of ROS, immune response, and phagocytosis (**Figure 2C**). By flow cytometry, we showed that cMO and iMO from DLBCL displayed a higher expression of CD64 and CCR2 ($P < .05$), without variation in HLA-DR and

CD163 (**Figure 2D**). Altogether, these results suggested that, in DLBCL, cMO and iMO share a common deregulated inflammatory phenotype.

DLBCL ncMO Are Decreased in Peripheral Blood and Exhibit an Inflammatory- and Tolerogenic-Like- Phenotype

We then focused on ncMO in DLBCL samples and found that both subsets of ncMO (ncMO Slan^{pos} and ncMO Slan^{neg}) were decreased in DLBCLs when compared to HDs [ncMO Slan^{pos} median at 3.3×10^6 cells/L vs 9.1×10^6 cells/L ($P < .001$) and ncMO Slan^{neg} median at 19×10^6 cells/L vs 23.7×10^6 cells/L ($P < .05$), respectively] (**Figure 3A**). No increase of apoptosis was detected in ncMO from DLBCL patients (data not shown). Then, sorted ncMO Slan^{pos} and ncMO Slan^{neg} from DLBCL and HD samples

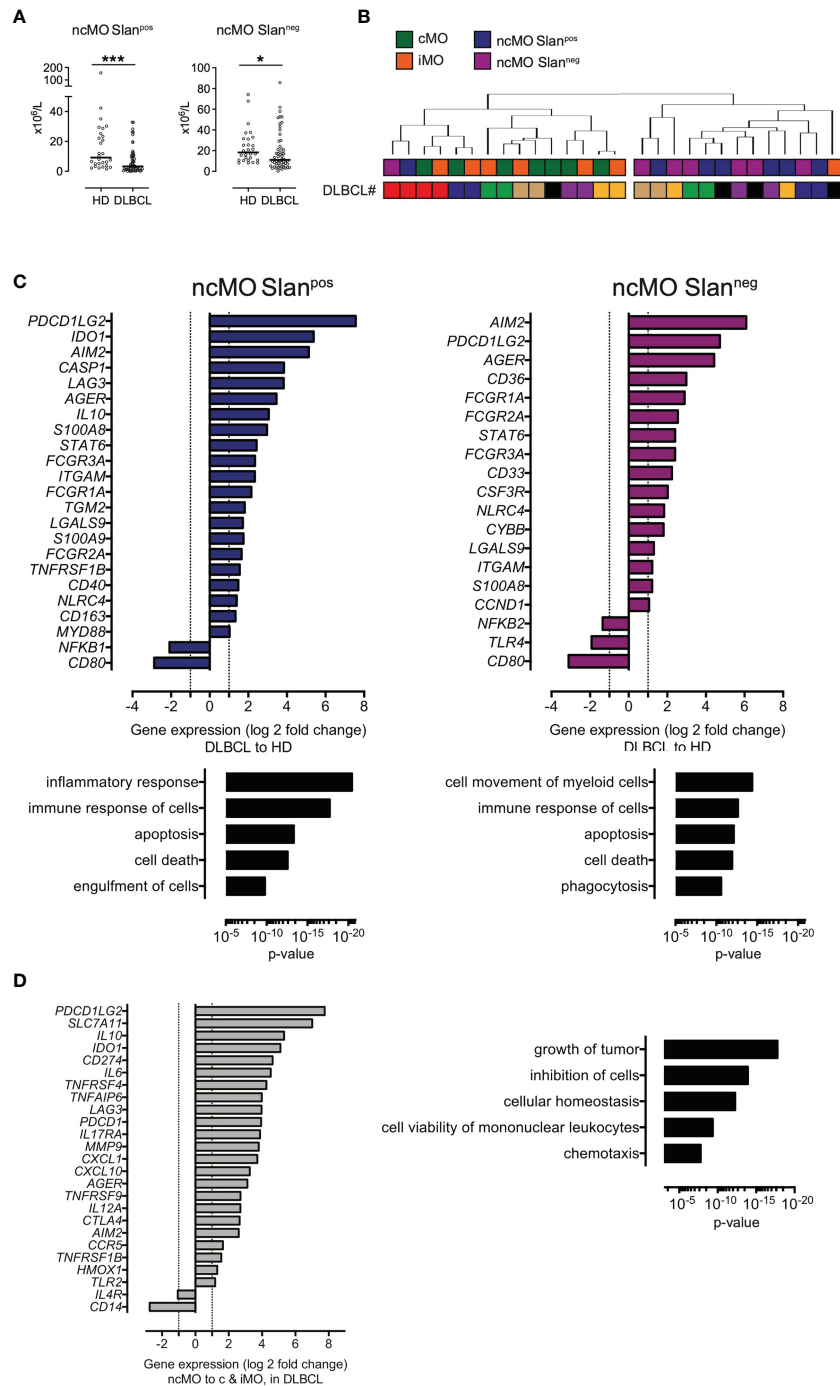


FIGURE 3 | ncMO are decreased in peripheral blood but exhibit an inflammatory- and tolerogenic- phenotype. **(A)** Nonclassical Slan^{pos} or Slan^{neg} (ncMOslan^{pos} and ncMOslan^{neg}) monocytes from HDs (n = 28) and DLBCLs (n = 56). Mann-Whitney test were performed. *P < .05, ***P < .001. **(B)** Unsupervised hierarchical clustering of classical- (cMO), intermediate- (iMO), nonclassical Slan^{pos}- or Slan^{neg}- (ncMOslan^{pos} and ncMOslan^{neg}) monocytes from DLBCL (n = 7) samples. DLBCL identity (#). List of genes analyzed on monocyte subsets after cell sorting is on **Table S3**. Pearson's correlation and complete linkage was employed. **(C)** Transcripts differentially expressed (P < .05; |log2FC| > 1) between DLBCLs (n=7) and HDs (n=4), for ncMO Slan^{pos} and ncMO Slan^{neg}. Predicted top 5 biological processes increased for ncMO Slan^{pos} and ncMO Slan^{neg} from DLBCL when compared to HD samples (Ingenuity Pathway Analysis, z-score > 2.5, ranked by p-value). **(D)** Transcripts (P < .05; |log2FC| > 1) enriched in ncMO compared to cMO and iMO for DLBCL. Predicted top 5 biological processes increased for ncMO compared to cMO and iMO, from DLBCL (Ingenuity Pathway Analysis, z-score > 2.5, ranked by p-value).

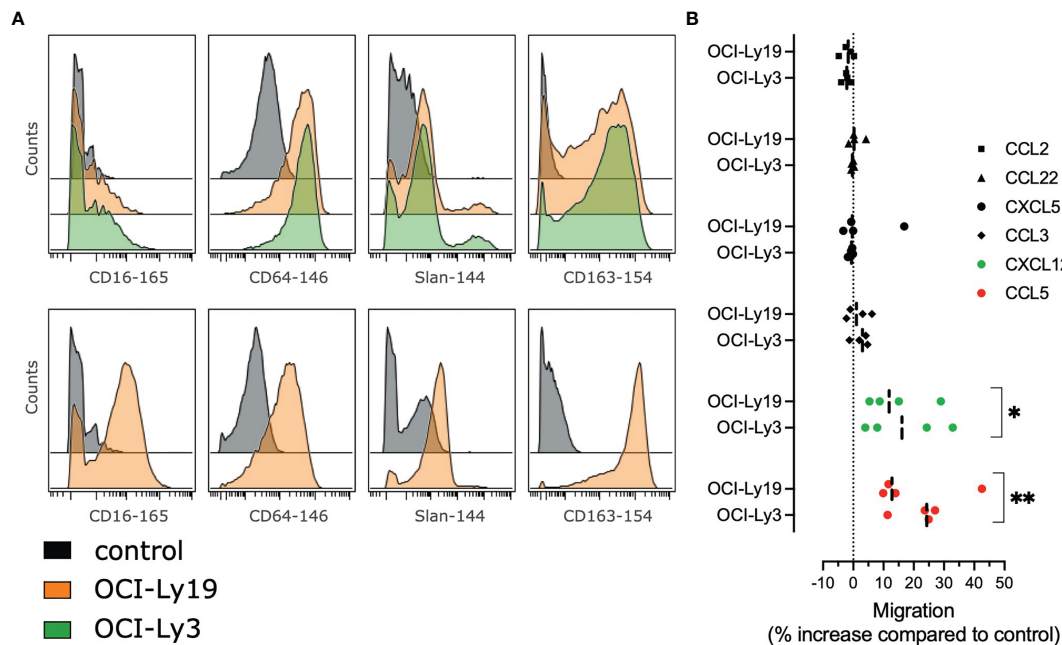


FIGURE 4 | Tumor cells supernatants polarize monocytes with higher migratory abilities. **(A)** Monocytes from healthy donors ($n = 2$) were treated with OCI-Ly3, OCI-Ly19 supernatant, or vehicle as control. Overlay histograms represent mean marker intensities for selected markers. Monocytes treated with vehicle (grey), OCI-Ly19 supernatant (orange), or OCI-Ly3 supernatant (green). Top: experiment 1. Bottom: experiment 2. **(B)** Migration assay for HD monocytes ($n = 4$) cultured or not with OCI-Ly3 and OCI-Ly19 supernatant in response to CCL2, CCL3, CCL5, CCL22, CXCL5, and CXCL12. Wilcoxon matched-pairs signed rank test were used to compare tumor-conditioned monocytes migration to the control condition (OCI-Ly medium). * $P < .05$, ** $P < .01$ (22).

were analyzed by high-throughput Q-PCR (**Figure S4**). To explore the similarities between ncMO Slan^{pos}, ncMO Slan^{neg}, iMO, and cMO, we performed an unsupervised hierarchical clustering on the DLBCL samples. For 6 out of 7 patients, cMO and iMO were separated from ncMO independently of Slan expression (**Figure 3B** and **Figure S5**). In addition, ncMO Slan^{pos} and ncMO Slan^{neg} exhibited tolerogenic genes (*PDCD1LG2*, *IL10*, *IDO*, *CD274*, *AGER*, *TNFAIP6*) (**Figure 3C** and **Figure S5**), most of these genes were not expressed in HD ncMO (**Figure S6**). In DLBCL, cMO and iMO in one hand and ncMO Slan^{pos} and ncMO Slan^{neg} in the other hand shared similar gene expression (**Figure 2A** and **Figure S5**), thus we compared the gene expression between ncMO, irrespectively of the Slan status, and both cMO and iMO. DLBCL ncMO were enriched for both inflammatory (*CXCL10*, *AIM2*, *IL12A*) and tolerogenic (*PDCD1LG2*, *IL10*, *IDO*, *CD274*, *AGER*) genes ($P < .05$, $|\log_2FC| > 1$) compared to cMO and iMO (**Figure 3C**). Biological processes involved by genes enriched in ncMO from DLBCL patients were growth of tumor, inhibition of cells, and chemotaxis (**Figures 3C, D**).

Tumor Conditioned Monocytes Give Rise to MO Prone to Migrate in Response to CCL5 and CXCL12

In order to evaluate how tumor B cells contribute directly to the phenotype of DLBCL monocytes, we cultured monocytes from

HD with supernatants from the DLBCL cell lines OCI-Ly3 and OCI-Ly19. After coculture, we analyzed the monocyte phenotype by mass cytometry (23, 25) and noticed an increased expression of CD16, Slan, CD64, CD163. We concluded that tumor conditioned monocytes triggered the cMO to ncMO transition (**Figure 4A**). Then we wondered if these cells were prone to migrate into tissue. Tumor-conditioned monocytes demonstrated an increase in *in vitro* migration in response to CCL5 and CXCL12 when compared to non-conditioned monocytes (**Figure 4B**).

High Level of Circulating ncMO Is Correlated With an Adverse Prognosis in DLBCL

Then, we evaluated the prognosis value of cMO, iMO, and ncMO in DLBCL. We used i) the proportion of ncMO to other monocytes (ratio ncMO to sum of cMO and iMO) and ii) the absolute count of circulating cMO, iMO, and ncMO. Analysis was performed on 52 patients for which clinical data were available. cMO and iMO were not associated with prognosis (data not shown). By contrast, patients with high proportion of ncMO and high absolute count of circulating ncMO were associated with a lower event-free survival probability ($P = .043$ and $P = .0061$, respectively) using thresholds (ratio at 0.06 and ncMO at 20.58×10^6 cells/L) defined with the maxstat package (**Figure 5A** and **Figure S7**). To validate the prognosis

value of ncMO obtained on this training cohort, we analyzed by flow cytometry the proportion of monocyte subsets in an independent cohort of 155 DLBCL samples from the recently published GAINED trial (NCT01659099) (24). With the previously calculated thresholds, high proportion of ncMO and high absolute count of ncMO was associated with a lower overall survival ($P = .017$ and $P = .011$, respectively) (**Figure 5A**). A univariate analysis on the validation cohort showed that Ann Arbor Stage III-IV, ECOG status >1 , elevated LDH, PET4 positivity, and increase in circulating ncMO were associated with lower OS (**Table 2**). In a multivariable analysis Ann Arbor Stage III-IV, PET4 positivity, increase in circulating ncMO remained statistically significant (**Table 2**). We previously demonstrated the accumulation of M-MDSC in DLBCL (22) and since no phenotypic overlap existed between

M-MDSC and ncMO (**Figure 1D**), we wondered if patients' characteristics were different between M-MDSC^{high} and ncMO^{high} DLBCLs. Both M-MDSC and ncMO were infrequently increased together [11 cases out of 155 (7.1%)]; ncMO were increased alone in 51 cases (32.9%), and M-MDSC were increased alone in 28 cases (18.1%) (**Figure 5B**). Interestingly, ncMO^{high} and M-MDSC^{high} patients corresponded to different types of patients. In particular when compared to ncMO^{low}, ncMO^{high} were enriched in ABC DLBCL subtypes [37.5 vs 15.9% ($P = .014$)] and in older patients [median age at 50 vs 46 years ($P = .044$)]. On the other hand, when compared to ncMO^{high}, M-MDSC^{high} patients were younger [median age at 42 vs 50 years ($P = .0027$)] and had higher levels of soluble PD-L1 [sPD-L1 at 1849 vs 1142 pg/mL ($P = .008$)] (**Figure 5B**).

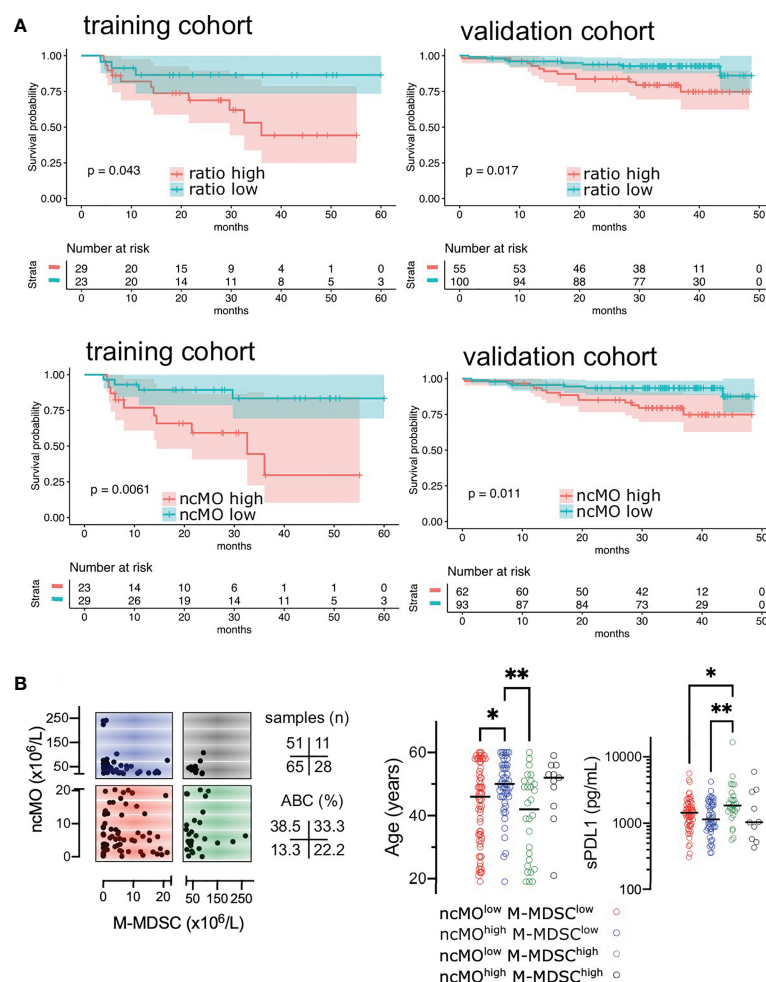


FIGURE 5 | High levels of circulating ncMO is correlated to adverse prognosis in DLBCL. **(A)** Event-free survival (EFS) in training cohorts (NCT01287923) and overall survival (OS) in validation cohorts (NCT01659099) (24). Patients were stratified on the ratio of ncMO to other monocytes (cMO and iMO) and on the absolute count of circulating ncMO. Threshold was defined on the training cohort using the maxstat package (**Figure S7**). Survival probability was calculated for both groups with a log-rank test. **(B)** Absolute count for ncMO (threshold at 20.58×10^6 cells/L) and M-MDSC (threshold at 22.51×10^6 cells/L) (22), and distribution of age and soluble PD-L1 (sPD-L1), * $P < .05$, ** $P < .01$.

TABLE 2 | Factors influencing overall survival in validation cohort.

| Risk factors | | N (%) | Univariate analysis | | Multivariate analysis | |
|----------------------------|----------------------|-------------|---------------------|--------------|-----------------------|--------------|
| | | | HR | P | HR | P |
| Age (years) | >50 | 59 (38.1%) | 1.096 | 0.84 | | |
| | ≤50 | 96 (61.9%) | | | | |
| Gender | Male | 86 (55.5%) | 1.027 | 0.952 | | |
| | Female | 69 (44.5%) | | | | |
| ECOG | ≥2 | 18 (11.6%) | 3.61 | 0.008 | 1.567 | 0.440 |
| | 0-1 | 137 (88.4%) | | | | |
| Ann Arbor stage | III-IV | 130 (83.9%) | 7.52 | 0.006 | 8.42 | 0.002 |
| | I-II | 25 (16.1%) | | | | |
| LDH | Elevated | 52 (34.4%) | 2.852 | 0.025 | 2.432 | 0.131 |
| | Normal | 99 (65.6%) | | | | |
| aalPI | 2-3 | 87 (56.1%) | 1.447 | 0.431 | | |
| | 0-1 | 68 (43.9%) | | | | |
| Bulk | ≥10 cm | 47 (30.3%) | 1.283 | 0.595 | | |
| | <10 cm | 108 (69.7%) | | | | |
| COO | ABC | 83 (74.8%) | 1.704 | 0.302 | | |
| | GCB | 28 (25.2%) | | | | |
| BCL2 | ≥70% | 87 (67.4%) | 0.5 | 0.283 | | |
| | <70% | 42 (32.6%) | | | | |
| MYC | ≥40% | 53 (46.5%) | 1.172 | 0.767 | | |
| | <40% | 61 (53.6%) | | | | |
| DE MYC/BCL2 | Yes | 45 (29.8%) | 0.847 | 0.75 | | |
| | No | 106 (70.2%) | | | | |
| Treatment arm | Obinutuzumab | 76 (49.4%) | 1.089 | 0.853 | | |
| | Rituximab | 78 (50.6%) | | | | |
| Chemotherapy | CHOP | 77 (50%) | 0.881 | 0.784 | | |
| | ACVBP | 77 (50%) | | | | |
| PET2/PET4 | PET4+ | 26 (19%) | 3.744 | 0.013 | 2.943 | 0.03 |
| | PET2- or PET2+/PET4- | 111 (81%) | | | | |
| ncMO (x10 ⁶ /L) | ≥20.58 | 62 (40%) | 3.135 | 0.015 | 3.362 | 0.047 |
| | <20.58 | 93 (60%) | | | | |

ECOG, Eastern Cooperative Oncology Group scale; LDH, lactate dehydrogenase; aalPI, age adjusted International prognostic index; COO, cell of origin; DE, double expressor; PET2, PET after cycle 2; PET4, PET after cycle 4; ncMO, non-classical monocyte.

Bold depict significant *p*-values.

DISCUSSION

Although the prognostic relevance of total monocyte count has been described in large cohorts of DLBCL in the last decade (11–15), few studies evaluated which particular monocyte subset was involved. In a previous work, we have shown an accumulation of M-MDSC (CD14^{pos} HLA-DR^{low}) in peripheral blood from DLBCL patients (22). Because M-MDSCs were not responsible for the whole increase in monocytes in our cohort, we explored cMO, iMO, and ncMO subsets. We demonstrated an increase in cMOs and iMOs in DLBCL, as in other lymphomas subtypes tested (CLL, MCL, MZL, and FL). In DLBCL, these MO subsets shared an inflammatory phenotype. By contrast, ncMOs were decreased in peripheral blood only in DLBCLs when compared to HDs or other B cell lymphomas. Interestingly, high number of circulating ncMO was an adverse prognosis in 2 independent cohorts of DLBCL patients. Finally, we found that tumor-conditioned monocytes shared a common phenotype with ncMOs and were prone to migrate in response to chemokines.

Surprisingly cMO and iMO from DLBCL showed common deregulated pathways with an enrichment for *FCGR3A*, *CD36*, *FCGR1A*, *CYBB*, *AIM2*, *STAT6*, *FCGR2A*, *CCR2*, *NLR4*, *S100A8*, and *CD14*. These genes are broadly expressed in cMO in healthy

samples (2, 5) and our results suggest that iMO and cMO are tumor-educated and polarized to a common inflammatory phenotype in DLBCL. In our study we found a decrease in both circulating ncMO Slan^{neg} and ncMO Slan^{pos} when compared to HDs, whereas an increase in ncMO Slan^{pos} was previously described in DLBCL (16). This discrepancy might be explained by differences in patient characteristics between both studies. In particular patients were older in the study from Verni et coll [63.9 years (range: 31–86) vs 50 years (range: 18–83)] and at higher grade (clinical stage III–IV at 80.5% vs 70% and IPI ≥3 at 55.6% vs 40%) (16). In CLL, an increase of ncMO correlates with high cytogenetic risk (deletion 11q, 17p, or trisomy 12) (28). In our study, an increase of the proportion of circulating ncMO was a worse prognosis factor in 2 independent cohorts. This was previously suggested on 45 DLBCLs where the decrease of CD16^{neg} monocyte to CD16^{pos} monocyte ratio predicted poor prognosis, however conclusions were limited because iMO and cMO were analyzed conjointly (17). ncMO abundance also predicted patient survival of pediatric and adult B acute lymphoblastic leukemia (29). Interestingly, in a pre-clinical mouse model of B cell lymphomas, Ly6C^{low} monocytes (corresponding to the ncMO) (30) accumulated and showed high levels of immunosuppressive genes (*PD-L1*, *PD-L2*, *Arg1*, *IDO1*, and *CD163*) associated with suppression of T cell proliferation (31).

In colorectal cancer Ly6C^{low} monocyte mediated immunosuppression by IL-10 production (32). Finally, ncMO were increased in gastric cancer (33). Conversely, in a lung cancer model, LyC^{low} monocytes recruited NK cells to prevent cancer metastasis (34). In DLBCL, we and others focused on total monocyte and on M-MDSC and few attentions were given to other monocyte subsets. Interestingly, ncMO and M-MDSC have non-overlapping phenotype regarding HLA-DR expression and these cells infrequently correlated in patients suggesting different mechanism of myelopoiesis dysregulation. Patients that were enriched in circulating MDSCs were younger and presented high amount of sPD-L1, a pejorative marker (35). Interestingly, release of PD-L1 was a mechanism of immune suppression suggested in DLBCL (22). Nonclassical monocytes have been associated age in healthy patients (36), however, no correlation was found in DLBCL samples between age and ncMO (data not shown).

Beside immunosuppression, gene enriched in ncMO were related to chemotaxis. Circulating ncMO are diminished in DLBCL, on the contrary there were enriched in other B cell lymphomas or solid tumor (37), thus we hypothesized that these cells might migrate into tissue to contribute to the tumor-associated macrophage compartment. CCL2, CCL3, CCL5, CCL22, CXCL5, and CXCL12 are involved in monocyte, MDSC, and macrophage recruitment into the TME (38). Tumor-conditioned monocyte shown an increased migration in response to CXCL5, CXCL12, CCL3, and CCL5. In our previous study, CXCL5 expression was increased in peripheral blood from DLBCL compared to healthy donors and its expression was related to a worse event-free survival (22). CCL3 is also increased in DLBCL when compared to HD and high level correlates with shorter survival (39, 40). CCL5 is involved in macrophage recruitment in DLBCL (41).

In DLBCL, TAM are heterogenous (23), in particular a Slan^{pos} macrophage subset is involved in rituximab mediated antibody dependent cellular cytotoxicity (16). In agreement, we found in DLBCL a compartment of cells expressing Slan at high level with CD14, CD32, and HLA-DR. However, DLBCL clusters that correlated with tumor-conditioned monocytes highly expressed CD64, CD36, and S100A9 and thus presented similarities with IFN γ *in-vitro* polarized macrophages (25). Few studies compared paired samples from circulating and *in situ* myeloid cells. In melanoma patient, myeloid cells obtained from the blood, but not from the tumor, were suppressive (42). In lung adenocarcinoma, macrophages phenotype detected in tumor were not present in peripheral blood (43). Currently, there is no model of lymphoma that allows tracking the myeloid cell from the blood to the tissues. Future studies entailing a prospective collection of paired blood and tumor samples are needed to confirm these observations on ncMO and to put in perspective the myeloid compartment with the T/NK compartment. Also, it would be interested to test the prognosis value in cohort of DLBCL treated with other immunotherapies and correlate with responders vs non-responders.

Our study as some limitations, in particular the lack of extensive functional studies due to the low number of circulating ncMO in DLBCL samples precluding large cell sorting. Data on gene expression in the monocyte subsets need

confirmation with cell preparations, for which a high purity is documented. Even if we previously identified CD16 macrophages subsets in DLBCL in dissociated tissue (23), additional studies with high dimensional spatial positioning of macrophage subsets will enrich our study. Finally, functional assays would be required to definitively address the suppressive activity of DLBCL ncMO for instance using mice models allowing to track the cMO to ncMO transition and the migration to tissue during the lymphoma course will also be valuable. Taken together, our results show that ncMO are involved in the DLBCL physiopathology and impact the prognosis of the disease. Given the current and our previous data, we propose that cMO and iMO are reflecting the inflammatory status in DLBCL, whereas M-MDSC are responsible of a systemic suppressive response, and ncMO are involved in suppressive response and migration to tissue.

DATA AVAILABILITY STATEMENT

The datasets presented in this study can be found in online repositories. The names of the repository/repositories and accession number(s) can be found below: <http://flowrepository.org/id/FR-FCM-Z4N6>.

ETHICS STATEMENT

The studies involving human participants were reviewed and approved by CHU Rennes. The patients/participants provided their written informed consent to participate in this study.

AUTHOR CONTRIBUTIONS

SGa, FL, AM, CM, and IA designed and performed experiments, analyzed data. JL, DR, JF, and TM analyzed data. CP, KB, GD, GC, PG, SGo, R-OC, RH, and TL provided samples. TF and KT raised the funds and analyzed data. MR designed and supervised research, analyzed data, and wrote the paper. All authors contributed to the article and approved the submitted version.

FUNDING

This work was supported by a fellowship from the Nuovo-Soldati Foundation (Switzerland) (MR), from the Ligue contre le Cancer (MR), from the COMITE de la REcherche Clinique et Translationnelle, CHU of Rennes (FL), from the Association pour le Développement de l'Hématologie Oncologie (FL), from the National Institute of Cancer (INCa Recherche Translationnelle 2010) (TF), from the Groupe Ouest-Est des Leucémies et des Autres Maladies du Sang (GOELAMS) (TF), from the Agence Nationale de la Recherche (ANR-17-CE15-0015 StroMAC) (KT), and from the Fondation ARC (PGA1 RF20190208534) (KT and MR).

ACKNOWLEDGMENTS

We are indebted to the clinicians of the BREHAT network and to the French Blood Bank (EFS) of Rennes for providing samples. The authors acknowledge the Centre de Ressources Biologiques (CRB-santé) of Rennes (BB-0033-00056) for managing samples and the Flow Cytometry facility, Biosit, University of Rennes 1 for cell sorting. This article was submitted as preprint (<https://www.biorxiv.org/content/10.1101/2021.04.10.439292v1>) (44).

SUPPLEMENTARY MATERIAL

The Supplementary Material for this article can be found online at: <https://www.frontiersin.org/articles/10.3389/fimmu.2021.755623/full#supplementary-material>

Figure S1 | Gating strategy.

Figure S2 | All monocyte subsets are increased in B-cell lymphomas A- Monocyte subsets counts in peripheral blood from HD (n = 6), follicular lymphomas (n = 9), mantle cell lymphomas (MCL, n = 9), chronic lymphocytic leukemias (CLL, n = 11), and marginal zone lymphomas (SMZL, n = 10). On these patients, flow cytometry was performed on cryopreserved cells. B- Ratio between MO (classical and intermediate) and ncMO in B-cell lymphomas.

Figure S3 | Q-PCR analysis, unsupervised hierarchical clustering for cMO and iMO from DLBCL and HD patients cMO and iMO were sorted from 7 DLBCL and 4

HD before analysis by high-throughput Q-PCR for genes listed in Table S3. Pearson's correlation and complete linkage were employed.

Figure S4 | Q-PCR analysis, unsupervised hierarchical clustering for ncMO Slanpos and ncMO Slanneg from DLBCL and HD patients ncMO Slanpos and ncMO Slanneg were sorted from 7 DLBCL and 4 HD before analysis by high-throughput Q-PCR for genes listed in Table S3. Pearson's correlation and complete linkage were employed.

Figure S5 | Q-PCR analysis, unsupervised hierarchical clustering for cMO, iMO, ncMO Slanpos and ncMO Slanneg from DLBCL patients cMO, iMO, ncMO Slanpos, and ncMO Slanneg were sorted from 7 DLBCL before analysis by high-throughput Q-PCR for genes listed in Table S3. Pearson's correlation and complete linkage were employed.

Figure S6 | Q-PCR analysis, unsupervised hierarchical clustering for cMO, iMO, ncMO Slanpos and ncMO Slanneg from DLBCL and HD patients cMO, iMO, ncMO Slanpos, and ncMO Slanneg were sorted from 7 DLBCL and 4 HD before analysis by high-throughput Q-PCR for genes listed in Table S3. Pearson's correlation and complete linkage were employed.

Figure S7 | High levels of circulating ncMO is an adverse event in DLBCL. Event-free survival (EFS) in training cohorts (NCT01287923) Threshold of the ratio of ncMO to other monocytes parameter was defined on the training cohort using the maxstat package.

Table S1 | Antibodies for fluorescent flow cytometry analysis.

Table S2 | Antibodies or parameters used for mass cytometry analysis.

Table S3 | List of genes evaluated by high-throughput Q-PCR on monocyte subsets.

Table S4 | QPCR data.

REFERENCES

- Ziegler-Heitbrock L, Ancuta P, Crowe S, Dalod M, Grau V, Hart DN, et al. Nomenclature of Monocytes and Dendritic Cells in Blood. *Blood* (2010) 116:e74–80. doi: 10.1182/blood-2010-02-258558
- Cros J, Cagnard N, Woollard K, Patey N, Zhang S-Y, Senechal B, et al. Human CD14dim Monocytes Patrol and Sense Nucleic Acids and Viruses via TLR7 and TLR8 Receptors. *Immunity* (2010) 33:375–86. doi: 10.1016/j.immuni.2010.08.012
- Ahmad F, Döbel T, Schmitz M, Schäkel K. Current Concepts on 6-Sulfo LacNAc Expressing Monocytes (slanMo). *Front Immunol* (2019) 10:948. doi: 10.3389/fimmu.2019.00948
- Bronte V, Brandau S, Chen S, Colombo MP, Frey AB, Greten TF, et al. Recommendations for Myeloid-Derived Suppressor Cell Nomenclature and Characterization Standards. *Nat Commun* (2016) 7:12150. doi: 10.1038/ncomms12150
- Wong KL, Tai JJ-Y, Wong W-C, Han H, Sem X, Yeap W-H, et al. Gene Expression Profiling Reveals the Defining Features of the Classical, Intermediate, and Nonclassical Human Monocyte Subsets. *Blood* (2011) 118:e16–31. doi: 10.1182/blood-2010-12-326355
- Guilliams M, Mildner A, Yona S. Developmental and Functional Heterogeneity of Monocytes. *Immunity* (2018) 49:595–613. doi: 10.1016/j.immuni.2018.10.005
- Lenz G, Wright G, Dave SS, Xiao W, Powell J, Zhao H, et al. Stromal Gene Signatures in Large-B-Cell Lymphomas. *N Engl J Med* (2008) 359:2313–23. doi: 10.1056/nejmoa0802885
- Riihijarvi S, Fiskvik I, Taskinen M, Vajavaara H, Tikka M, Yri O, et al. Prognostic Influence of Macrophages in Patients With Diffuse Large B-Cell Lymphoma: A Correlative Study From a Nordic Phase II Trial. *Haematologica* (2015) 100:238–45. doi: 10.3324/haematol.2014.113472
- Scott DW, Gascoyne RD. The Tumour Microenvironment in B Cell Lymphomas. *Nat Rev Cancer* (2014) 14:517–34. doi: 10.1038/nrc3774
- Nam SJ, Kim S, Kwon D, Kim H, Kim S, Lee E, et al. Prognostic Implications of Tumor-Infiltrating Macrophages, M2 Macrophages, Regulatory T-Cells, and Indoleamine 2,3-Dioxygenase-Positive Cells in Primary Diffuse Large B-Cell Lymphoma of the Central Nervous System. *Oncoimmunology* (2018) 7:1–39. doi: 10.1080/2162402x.2018.1442164
- Tadmor T, Bari A, Sacchi S, Marcheselli L, Liardo EV, Avivi I, et al. Monocyte Count at Diagnosis Is a Prognostic Parameter in Diffuse Large B-Cell Lymphoma: Results From a Large Multicenter Study Involving 1191 Patients in the Pre- and Post-Rituximab Era. *Haematologica* (2014) 99:125–30. doi: 10.3324/haematol.2013.088161
- Nitta H, Terui Y, Yokoyama M, Mishima Y, Nishimura N, Ueda K, et al. Absolute Peripheral Monocyte Count at Diagnosis Predicts Central Nervous System Relapse in Diffuse Large B-Cell Lymphoma. *Haematologica* (2015) 100:87–90. doi: 10.3324/haematol.2014.114934
- Tropan K, Deutsch A, Gerger A, Stojakovic T, Beham-Schmid C, Wenzl K, et al. The Derived Neutrophil to Lymphocyte Ratio Is an Independent Prognostic Factor in Patients With Diffuse Large B-Cell Lymphoma. *Br J Cancer* (2014) 110:369–74. doi: 10.1038/bjc.2013.763
- Wilcox RA, Ristow K, Habermann TM, Inwards DJ, Micallef INM, Johnston PB, et al. The Absolute Monocyte and Lymphocyte Prognostic Score Predicts Survival and Identifies High-Risk Patients in Diffuse Large-B-Cell Lymphoma. *Leukemia* (2011) 25:1502–9. doi: 10.1038/leu.2011.112
- Maurer MJ, Jais J-P, Ghesquière H, Witzig TE, Hong F, Haioun C, et al. Personalized Risk Prediction for Event-Free Survival at 24 Months in Patients With Diffuse Large B-Cell Lymphoma. *Am J Hematol* (2016) 91:179–84. doi: 10.1002/ajh.24223
- Vermi W, Micheletti A, Finotti G, Tecchio C, Calzetti F, Costa S, et al. Slan+ Monocytes and Macrophages Mediate CD20-Dependent B-Cell Lymphoma Elimination via ADCC and ADCP. *Cancer Res* (2018) 78:3544–59. doi: 10.1158/0008-5472.can-17-2344
- Han X, Ruan J, Zhang W, Zhou D, Xu D, Pei Q, et al. Prognostic Implication of Leucocyte Subpopulations in Diffuse Large B-Cell Lymphoma. *Oncotarget* (2017) 8:47790–800. doi: 10.18632/oncotarget.17830
- Yhim H-Y, Kim J-A, Ko S-H, Park Y, Yim E, Kim HS, et al. The Prognostic Significance of CD11b+CX3CR1+ Monocytes in Patients With Newly Diagnosed Diffuse Large B-Cell Lymphoma. *Oncotarget* (2017) 8:92289–99. doi: 10.18632/oncotarget.21241

19. Vari F, Arpon D, Keane C, Hertzberg MS, Talaulikar D, Jain S, et al. Immune Evasion via PD-1/PD-L1 on NK Cells and Monocyte/Macrophages Is More Prominent in Hodgkin Lymphoma Than DLBCL. *Blood* (2018) 131:1809–19. doi: 10.1182/blood-2017-07-796342
20. Lin Y, Gustafson MP, Bulur PA, Gastineau DA, Witzig TE, Dietz AB. Immunosuppressive CD14+HLA-DRlow/- Monocytes in B-Cell Non-Hodgkin Lymphoma. *Blood* (2011) 117:872–81. doi: 10.1182/blood-2010-05-283820
21. Xiu B, Lin Y, Grote DM, Ziesmer SC, Gustafson MP, Maas ML, et al. IL-10 Induces the Development of Immunosuppressive CD14(+)/HLA-DR(low/-) Monocytes in B-Cell Non-Hodgkin Lymphoma. *Blood Cancer J* (2015) 5:e328. doi: 10.1038/bcj.2015.56
22. Azzaoui I, Uhel F, Rossille D, Pangault C, Dulong J, Priol JL, et al. T-Cell Defect in Diffuse Large B-Cell Lymphomas Involves Expansion of Myeloid-Derived Suppressor Cells. *Blood* (2016) 128:1081–92. doi: 10.1182/blood-2015-08-662783
23. Roussel M, Lhomme F, Roe CE, Bartkowiak T, Gravelle P, Laurent C, et al. Mass Cytometry Defines Distinct Immune Profile in Germinal Center B-Cell Lymphomas. *Cancer Immunol Immunother* (2020) 69:407–20. doi: 10.1007/s00262-019-02464-z
24. Gouill SL, Ghesquière H, Oberic L, Morschhauser F, Tilly H, Ribrag V, et al. Obinutuzumab vs Rituximab for Advanced DLBCL: A PET-Guided and Randomized Phase 3 Study by LYSA. *Blood* (2021) 137:2307–20. doi: 10.1182/blood.2020008750
25. Roussel M, Ferrell PB, Greenplate AR, Lhomme F, Gallou SL, Diggins KE, et al. Mass Cytometry Deep Phenotyping of Human Mononuclear Phagocytes and Myeloid-Derived Suppressor Cells From Human Blood and Bone Marrow. *J Leukocyte Biol* (2017) 102:437–47. doi: 10.1189/jlb.5ma1116-457r
26. Roussel M, Bartkowiak T, Irish JM. Picturing Polarized Myeloid Phagocytes and Regulatory Cells by Mass Cytometry. *Methods Mol Biol* (2019) 1989:217–26. doi: 10.1007/978-1-4939-9454-0_14
27. Ferrant J, Lhomme F, Gallou SL, Irish JM, Roussel M. Circulating Myeloid Regulatory Cells: Promising Biomarkers in B-Cell Lymphomas. *Front Immunol* (2021) 11:623993. doi: 10.3389/fimmu.2020.623993
28. Maffei R, Bulgarelli J, Fiorcari S, Bertonecchi L, Martinelli S, Guarnotta C, et al. The Monocytic Population in Chronic Lymphocytic Leukemia Shows Altered Composition and Deregulation of Genes Involved in Phagocytosis and Inflammation. *Haematologica* (2013) 98:1115–23. doi: 10.3324/haematol.2012.073080
29. Witkowski MT, Dolgalev I, Evensen NA, Ma C, Chambers T, Roberts KG, et al. Extensive Remodeling of the Immune Microenvironment in B Cell Acute Lymphoblastic Leukemia. *Cancer Cell* (2020) 37:867–82.e12. doi: 10.1016/j.ccell.2020.04.015
30. Ginhoux F, Jung S. Monocytes and Macrophages: Developmental Pathways and Tissue Homeostasis. *Nat Rev Immunol* (2014) 14:392–404. doi: 10.1038/nri3671
31. McKee SJ, Tuong ZK, Kobayashi T, Doff BL, Soon MS, Nissen M, et al. B Cell Lymphoma Progression Promotes the Accumulation of Circulating Ly6Clo Monocytes With Immunosuppressive Activity. *Oncoimmunology* (2018) 7:e1393599. doi: 10.1080/2162402x.2017.1393599
32. Jung K, Heishi T, Khan OF, Kowalski PS, Incio J, Rahbari NN, et al. Ly6Clo Monocytes Drive Immunosuppression and Confer Resistance to Anti-VEGFR2 Cancer Therapy. *J Clin Invest* (2017) 127:3039–51. doi: 10.1172/jci93182
33. Eljaszewicz A, Jankowski M, Gackowska L, Helmin-Basa A, Wiese M, Kubiszewska I, et al. Gastric Cancer Increase the Percentage of Intermediate (CD14++CD16+) and Nonclassical (CD14+CD16+) Monocytes. *Clin Immunol* (2012) 4:355–61. doi: 10.5114/ceji.2012.32725
34. Hanna RN, Cekic C, Sag D, Tacke R, Thomas GD, Nowyhed H, et al. Patrolling Monocytes Control Tumor Metastasis to the Lung. *Science* (2015) 350:985–90. doi: 10.1126/science.aac9407
35. Rossille D, Azzaoui I, Feldman AL, Maurer MJ, Labouré G, Parrens M, et al. Soluble Programmed Death-Ligand 1 as a Prognostic Biomarker for Overall Survival in Patients With Diffuse Large B-Cell Lymphoma: A Replication Study and Combined Analysis of 508 Patients. *Leukemia* (2017) 31:988–91. doi: 10.1038/leu.2016.385
36. Ong SM, Hadadi E, Dang TM, Yeap W-H, Tan CT-Y, Ng T-P, et al. The Pro-Inflammatory Phenotype of the Human Non-Classical Monocyte Subset Is Attributed to Senescence. *Cell Death Dis* (2018) 9(3):266. doi: 10.1038/s41419-018-0327-1
37. Cassetta L, Fragiogianni S, Sims AH, Swierczak A, Forrester LM, Zhang H, et al. Human Tumor-Associated Macrophage and Monocyte Transcriptional Landscapes Reveal Cancer-Specific Reprogramming, Biomarkers, and Therapeutic Targets. *Cancer Cell* (2019) 35:588–602.e10. doi: 10.1016/j.ccell.2019.02.009
38. Nagarsheth N, Wicha MS, Zou W. Chemokines in the Cancer Microenvironment and Their Relevance in Cancer Immunotherapy. *Nat Rev Immunol* (2017) 17:559–72. doi: 10.1038/nri.2017.49
39. Charbonneau B, Maurer MJ, Ansell SM, Slager SL, Fredericksen ZS, Ziesmer SC, et al. Pretreatment Circulating Serum Cytokines Associated With Follicular and Diffuse Large B-Cell Lymphoma: A Clinic-Based Case-Control Study. *Cytokine* (2012) 60:882–9. doi: 10.1016/j.cyto.2012.08.028
40. Takahashi K, Sivina M, Hoellenriegel J, Oki Y, Hagemeyer FB, Fayad L, et al. CCL3 and CCL4 Are Biomarkers for B Cell Receptor Pathway Activation and Prognostic Serum Markers in Diffuse Large B Cell Lymphoma. *Brit J Haematol* (2015) 171:726–35. doi: 10.1111/bjh.13659
41. Manfroi B, Grandis MD, Moreaux J, Tabruyn SP, Mayol J-F, Quintero M, et al. The Microenvironment of DLBCL Is Characterized by Non-Canonical Macrophages Recruited by Tumor-Derived CCL5. *Blood Adv* (2021) 5(21):4338–51. doi: 10.1182/bloodadvances.2021004203
42. Gros A, Turcotte S, Wunderlich JR, Ahmadzadeh M, Dudley ME, Rosenberg SA. Myeloid Cells Obtained From the Blood But Not From the Tumor Can Suppress T-Cell Proliferation in Patients With Melanoma. *Clin Cancer Res* (2012) 18:5212–23. doi: 10.1158/1078-0432.ccr-12-1108
43. Lavin Y, Kobayashi S, Leader A, Amir ED, Elefant N, Bigenwald C, et al. Innate Immune Landscape in Early Lung Adenocarcinoma by Paired Single-Cell Analyses. *Cell* (2017) 169:750–7.e15. doi: 10.1016/j.cell.2017.04.014
44. Gallou SL, Lhomme F, Irish JM, Mingam A, Pangault C, Monvoisin C, et al. Nonclassical Monocytes Are Prone to Migrate Into Tumor in Diffuse Large B-Cell Lymphoma. *Biorxiv* (2021). doi: 10.1101/2021.04.10.439292

Conflict of Interest: The authors declare that the research was conducted in the absence of any commercial or financial relationships that could be construed as a potential conflict of interest.

Publisher's Note: All claims expressed in this article are solely those of the authors and do not necessarily represent those of their affiliated organizations, or those of the publisher, the editors and the reviewers. Any product that may be evaluated in this article, or claim that may be made by its manufacturer, is not guaranteed or endorsed by the publisher.

Copyright © 2021 Le Gallou, Lhomme, Irish, Mingam, Pangault, Monvoisin, Ferrant, Azzaoui, Rossille, Bouabdallah, Damaj, Cartron, Godmer, Le Gouill, Casasnovas, Molina, Houot, Lamy, Tarte, Fest and Roussel. This is an open-access article distributed under the terms of the Creative Commons Attribution License (CC BY). The use, distribution or reproduction in other forums is permitted, provided the original author(s) and the copyright owner(s) are credited and that the original publication in this journal is cited, in accordance with accepted academic practice. No use, distribution or reproduction is permitted which does not comply with these terms.